Ring-Size Memory of Galactose-Containing MS/MS Fragments: Application to the Detection of Galactofuranose in Oligosaccharides and Their Sequencing

Oznur Yeni, Simon Ollivier, Baptiste Moge, David Ropartz, Hélène Rogniaux, Laurent Legentil, Vincent Ferrières, Isabelle Compagnon

Ring-Size Memory of Galactose-Containing MS/MS Fragments: Application to the Detection of Galactofuranose in Oligosaccharides and Their Sequencing

Oznur Yeni, Simon Ollivier, Baptiste Moge, David Ropartz, Hele`ne Rogniaux, Laurent Legentil, Vincent Ferrie`res, and Isabelle Compagnon*

ABSTRACT: Analysis of glycans remains a difficult task due to their isomeric complexity. Despite recent progress, determining monosaccharide ring size, a type ofsomerism, is still challenging due to the high flexibility of the five-membered ring (alsocalled furanose). Galactose is a monosaccharide that can be naturally found in furanose configuration in plant and bacterial polysaccharides. In this study, we used the coupling of tandem mass spectrometry and infrared ion spectroscopy (MS/MS-IR) to investigate compounds containing galactofuranose and galactopyranose. We report the IR fingerprints of monosaccharide fragments and demonstrate for the first time galactosering-size memory upon collision-induced dissociation (CID) conditions. The linkage of the galactose unit is further obtained by analyzing disaccharide fragments. These findings enable two possible applications. First, labeled oligosaccharide patterns can be analyzed by MS/MS-IR, yielding full sequence information, including the ring size of the galactose unit; second, MS/MS-IR can be readily applied to unlabeled oligosaccharides to rapidly identify the presence of a galactofuranose unit, as a standalone analysis or
prior to further sequencing.

INTRODUCTION

Galactose is a common hexose in natural carbohydrates and may be present in pyranose (6-membered ring) or furanose form (five-membered ring). Mammals only synthesize galactose units with pyranose configuration, which can be found for example in milk oligosaccharides or ABO blood group antigens.[1] The galactofuranose form is restricted to specific organisms such as bacteria, parasites, fungi, plants, and lichens.[2−4] Interestingly, the galactofuranose form is present in both pathogenic and nonpathogenic organisms presence of galactofuranose, which makes the study of the biosynthesis of the furanose form very interesting for the development of therapeutic targets and gaining a better understanding of the structure/activity relationship of this rare monosaccharide.[5,6]

Galactofuranose is naturally linked to other monosaccharides (mannose, glucose, N-acetylgalactosamine, fructose, etc.) in α-or β-configurations and can be found at the nonreducing end or as internal units of various glycans or glycoconjugates, thus Gal*f*-containing carbohydrates have a broad structural diversity. For example, ***Klebsiella pneumoniae*** produces a polysaccharide with a repeating unit β-D-Gal*f*-(1 → 3)-D-Gal*p*;[7] the peptidogalactomannan of ***Aspergillus fumigatus*** contains terminal β-Gal*f*-(1 → 5)-β-Gal*f groups*;[8] the disaccharide α-D-Gal*f*-(1-6)-α-D-Man form branches on the α-D-mannopyranosyl chain of ***Paracoccidioides brasiliensis***;[9] and β-D-galactofuranose is linked to the α-D-mannopyranosyl chain of some lichens.[10−13]

The biological interest of this rare sugar stimulates the development of analytical tools that enable one to fully characterize carbohydrate sequences, including the galactose ring size. Such glycomics developments include challenging carbohydrate synthesis of oligosaccharide standards to validate analytical methods. In this context, substantial efforts have been made to synthesize Gal*f*-containing compounds. A number of *β*-linked galactofuranose-containing oligosaccharides have been reported, such as disaccharides with the galactofuranose at the nonreducing end,[14,15] and trisaccharides with an internal galactofuranose moiety.[16] The synthesis of *α*-galactofuranosides-containing compounds is more challenging[17] and only very few *α*-Gal*f*-containing compounds have been reported.[18−20] In the past 10 years, tremendous efforts have been deployed to augment mass spectrometric approaches with ion mobility (IM-MS) and/or IR laser spectroscopy (MS-IR). Such couplings enable isomer identification, which is critical for glycomics.[21−28] These techniques are highly complementary: IMS-MS offers ion separation and collision cross-sectional data, and MS-IR brings an additional level of structural characterization. The 3 μm spectral range corresponds to OH, NH, and CH vibrations (elongation modes) and offers very distinctive fingerprints of monosaccharide isomers. The far-IR region can also be used to gain information on functional groups involving heavier atoms (S, P). Three types of IR ion spectroscopy schemes have been successfully used to obtain IR fingerprints of glycan ions. The IR spectroscopy in helium droplets is based on the encapsulation of the ion of interest in helium nanodroplets. Then, the droplets are irradiated with an IR laser, and helium atoms can evaporate.[27,29] Messenger-tagging IR spectroscopy consists of complexing the ion of interest to a messenger at a low temperature, which dissociates upon the absorption to one IR photon.[30,31] Finally, IRMPD (infrared multiple photon dissociation) consists of the resonant absorption of multiple IR photons, resulting in the photofragmentation of ions, which is monitored by the MS detector.[32−34]

For analytical applications, the MS-IR spectra can be obtained at various stages of MS_n acquisition. When the IR data are acquired on a precursor ion, the spectrum is directly compared with a database of measurements performed on ions that have the same mass-to-charge ratio (m/z) to identify its structure. This was successfully applied for various carbohydrate structure determination on mono- and disaccharides.[33,35] The analysis of galactofuranose-containing oligosaccharides is however a peculiar challenge because furanoses are known to be highly flexible,[36] which requires an analytical workflow that is able to conserve such elusive structural information. Recently, IRMPD and ion mobility spectrometry successfully defined galactofuranose-containing mono- or disaccharides by analyzing precursor mono- and disaccharide ions.[14,15,37] These studies have established the conservation of the galactose ringsize information during the gas-phase transfer. The major drawback of this approach is its lack of applicability to larger oligosaccharides. Indeed, the number of possible sequences strongly increases with the number of monomers,[38] which is rapidly unattainable by chemical synthesis. Alternatively, IRMPD spectra can be collected on fragment ions after MS/MS fragmentation. The fragmentation approach is more suitable in the case of larger compounds, providing structural information on MS fragments. Collision-induced dissociation (CID) is commonly used in glycomics and mainly results in glycosidic bond cleavage. The resulting set of the IRMPD data is then

analyzed and in-depth oligosaccharide sequence information is obtained by assembling fragments data using a reduced library of standards.[23,32] To access the ring-size information in larger oligosaccharides, the fragmentation approach could be envisioned, which requires the investigation of the impact of CID on the highly flexible furanose ring. We have recently reported promising IM-MS results on the fragmentation of galactose-containing trisaccharides, where the Gal-Man disaccharide fragment retained its structure in some conditions.[39] To validate the sequencing approach, it is thus essential to generalize the conservation of the ring-size structural features upon CID fragmentation, particularly in monosaccharide fragments. To address this question, we drew on patterns found in lichen polysaccharides (PS), which are nonpathogenic and relatively abundant. Previous works have identified lichenic galactomannan composed of a mannan backbone with branched *β*-D-galactofuranose at positions 2, 3, 4, or 6.[10−13] They contain a number of oligosaccharides patterns with galactose at the nonreducing end (Scheme 1).

Scheme 1. (a) Typical Structure of Lichen Galactomannan. (b) Example of Oligosaccharides Patterns Found in Lichen PS

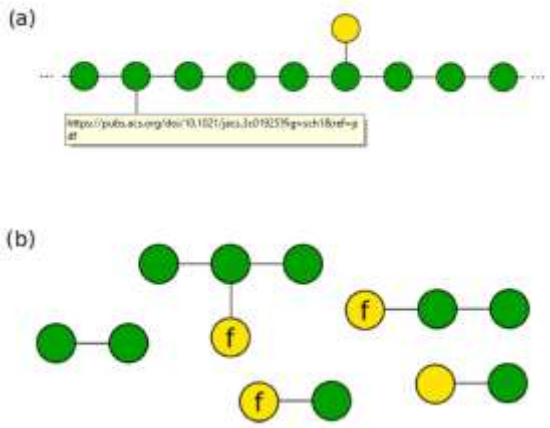

We used these patterns as models for the synthesis of an exhaustive library of galactomannan disaccharides and trisaccharide standards.[15] In the present work, we used these synthetic standards to establish the IR diagnostic of the ring size of galactose fragments produced by CID to validate the feasibility of the sequencing approach in the particular context of the description of the ring size. Disaccharides served to create a database containing *m/z* and IRMPD fingerprints of precursor and product ions. The relevance of the fragment choice for sequencing is discussed. MS/MS-IR was used to fully characterize a galactofuranose-containing trisaccharide, thus validating the MS/MS-IR approach to sequence galactofuranose-containing oligosaccharides. Finally, we present a simplified MS/MS-IR approach that allows us to rapidly detect the presence of galactofuranose in an oligosaccharide, without characterizing its other features.

EXPERIMENTAL SECTION

Chemical Library. The chemical library (Scheme 2) contains eight Gal-Man disaccharides mimicking patterns found in lichen polysaccharides, with galactose in pyranose (**1**−**4**) and furanose configuration (**5**−**8**). These disaccharides were also labeled with a thiophenyl group at the reducing end (**9**−**16**). The collection comprises two Man-Man disaccharides (**17** and **18**). Four linear Gal-Man-Man trisaccharides (**19**−**22**), whose structures are biologically relevant, were used to validate the sequencing approach using IRMPD.

The synthesis of disaccharides and disaccharides-SPh was previously described and structurally validated by NMR.[15] The synthesis of trisaccharides was validated by NMR and will be published elsewhere.

Sample Preparation. Water-^{18}O (97 atom % ^{18}O) was purchased from Sigma. Trisaccharides were ^{18}O labeled by drying 50 μL of each solution at 2 mg/mL and resuspending in 50 μL of $H_2{}^{18}O$. The samples were incubated at room temperature for at least one week. Disaccharides, disaccharides-SPh, and trisaccharides ^{18}O were prepared in water/methanol (50:50) at a concentration of 1 μg/mL, followed by adding LiCl (0.1%) to the solution to promote the Li^+ adduct formation.

IRMPD Signature Acquisition. The setup used to perform MS/IR and MS-MS/IR analysis was previously described.[40] A Thermofisher LTQ mass spectrometer equipped with an electrospray source ionization (ESI) is used to produce ions, which are then led to a linear ion trap. Helium serves as a collision gas for MS/MS analysis. A mass spectrometer was customized to allow irradiation of the trapped ions. Laser pulses are delivered by a YAG-pumped tunable OPO/OPA IR laser system (10 mJ/pulse, 10 Hz repetition rate) in the spectral range of 3300−3700 cm^{-1}. If the wavelength of the laser excitation corresponds to a vibrational mode of the irradiated ion, the ion accumulates internal energy from the light and then relaxes by photofragmentation. The photofragmentation yield is then recorded as the function of the wavenumber to obtain an IRMPD spectrum.

The samples were infused and ionized by ESI in positive mode to yield ions with an Li^+ adduct. The ions of a chosen m/z were isolated in the ion trap. To acquire the IRMPD spectra of disaccharides with lithium adduct, the ions at m/z 349 were isolated and irradiated during 400 ms. To analyze the fragments, the precursor ion (disaccharide-SPh or trisaccharide-^{18}O) was isolated during 30 ms and fragmented by CID. Then, the fragment of interest was isolated and irradiated by the laser for 700 ms (or 400 ms for fragments m/z = 349).

Scheme 2. Schematic Representation of Synthetic Standards with Symbol Nomenclature: Galactopyranose (Gal*p*) Represented with Yellow Circle, Galactofuranose (Gal*f*) with Yellow Circle Annotated with *f*, and Mannopyranose with Green Circle

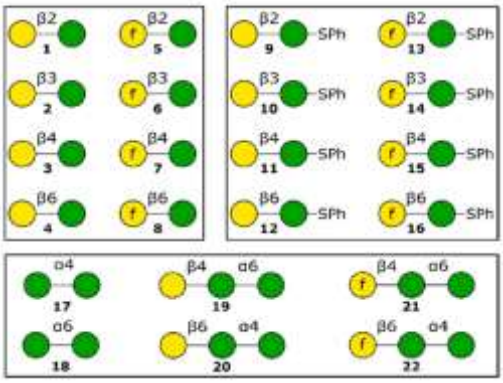

RESULTS AND DISCUSSION

MS/MS Fragments. The Domon and Costello nomenclature is used to describe fragments observed upon CID.[41] B and C types designate ions containing the nonreducing end, whereas Z and Y types contain the reducing end. B- and C-type ions are thus fragments of interest because they contain the galactose moiety (see Scheme 3). A constraint to studying molecules **1**−**8** and **19**−**22** is their symmetric structure, which implies that their reducing and nonreducing end fragments have the same mass. For example, B_1 and Z_1 fragments of **1**−**8** have both M = 162. The IRMPD spectra are obtained on trapped ions isolated according to their m/z ratio. It is thus essential to isolate only galactosecontaining fragments. We adopted two strategies to remove the symmetry. For disaccharides, intermediates of synthesis with a thiophenyl group at the reducing end were available (molecules **9**−**16**). This results in a shift of m/z 92 between B_1/Z_1 fragments and thus between C_1/Y_1 fragments (Scheme 3). Molecules **9**−**16** with a lithium adduct were detected at m/z 441 (Figure S1). The MS/MS spectrum shows B_1 detected at m/z 169, C_1 at m/z 187, Y_1 at m/z 279,

and the fragment corresponding to the loss of SPh at *m/z* 331. Trisaccharides (**19**–**22**) were labeled with ^{18}O to distinguish the reducing end from the nonreducing end. It is known that ^{18}O is incorporated at the reducing OH group, this results in a difference of 2 Da (Scheme 3, right panel). ^{18}O-labeled **19**–**22** with a lithium adduct were detected at *m/z* 513 (Figure S2) and the fragments of interest are *m/z* 169 (B_1), 187 (C_1), 189 (Y_1), 331 (B_2), 349 (C_2), and 351 (Y_2).

Scheme 3. Fragments Used in This Study: B_1 Fragments of Disaccharides-SPh and Trisaccharides-^{18}O (Figure 1); C_1 Fragments of Disaccharides-SPh and Trisaccharides-^{18}O (Figure S3); Disaccharides-SPh with the Loss of SPh Group Fragments and B_2 Fragments of Trisaccharides-^{18}O (Figure 2); Man-Man Disaccharides and Y_2 Fragments of Trisaccharides-^{18}O (Figure 4)[a]

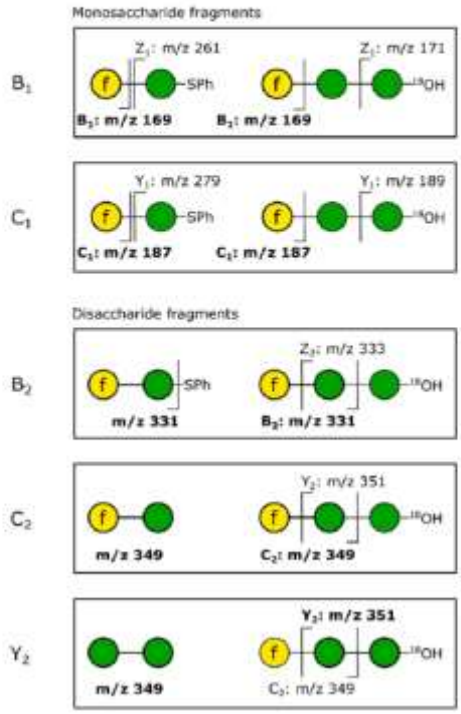

[a] Only galactofuranose-containing molecules are represented; the measurements were also performed on their galactopyranose counterparts.

Disaccharides and trisaccharides displayed common glycosidic linkage fragments that are gathered in Scheme 3. Our approach consists of the comparison of their IRMPD spectra to validate the conservation of the ring-size information after fragmentation and the applicability of the IR sequencing method.

Identification of the Ring Size in Galactose Monosaccharide Fragments. Two monosaccharide fragments can be detected for compounds **9**–**16**, **20**, and **22** with a lithium adduct: B_1 at *m/z* 169 and C_1 at *m/z* 187, which correspond to dehydrated and intact galactose, respectively. The IRMPD spectra of the B_1 fragments are displayed in the range of 3300–3700 cm^{-1} in Figure S3. Both galactofuranose and galactopyranose B_1 fragments show an intense band around 3650 cm^{-1}, corresponding to free OH, which does not allow us to distinguish them. However, the range corresponding to the bound OH (3350–3550 cm^{-1}) is more distinctive and represented in Figure 1. For Gal*f*-ManSPh compounds (**13**–**16**), the B_1 spectra show a region of vibrational activity. from 3350 to 3475 cm^{-1}

and not from 3475 to 3550 cm^{-1}. Interestingly, their galactopyranose counterparts (**9**–**12**) present the opposite: a vibrational band from 3475 to 3550 cm^{-1} and not from 3350 to 3475 cm^{-1}. These features are also verified on B_1 fragments of trisaccharides (bottom panel in Figure 1). Thus, all investigated molecules exhibit a strong diagnostic in this region, and the bands at 3410 and 3510 cm^{-1} are very specific to the galactose ring size. The C_1 fragments were also investigated and their IRMPD signatures can be distinguished, although with less contrast (Figure S3).

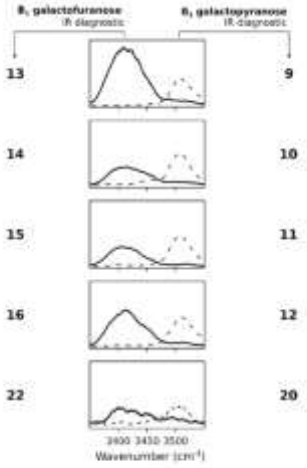

Figure 1. B_1 fragment IR fingerprints of galactofuranose-containing compounds: 13–16 and ^{18}O-labeled **22** (solid line). B_1 fragment IR fingerprints of galactopyranose-containing compounds: 9–12 and ^{18}O-labeled **20** (dashed line). The position of the two diagnostic bands is shaded in gray.

These results are remarkable because they suggest that the monosaccharide fragments conserve galactose ring-size information upon fragmentation, even after the molecular rearrangement caused by the cleavage of the C1–O1 bond. This implies that the galactose ring size in oligosaccharides can be determined by the spectroscopic analysis of the monosaccharide fragments. This approach presents the advantage of requiring only two reference spectra and can be applied for oligosaccharides with different sizes and linkage positions. Another benefit is the narrow range of laser wavenumbers required to distinguish these two signatures. This range can be quickly scanned, which reduces the acquisition time and therefore the time for ring-size diagnostic.

Identification of the Ring Size and Linkage Type in Disaccharide Fragments. The linkage position can be further described by comparison with reference disaccharide patterns. To assess the linkage position of Gal-Man disaccharide, nonreducing end disaccharide fragments are analyzed. Fragments *m/z* 331 of Gal-ManSPh have been collected to create a database of IRMPD spectra, which are represented in color in Figure 2. For Gal*p*-ManSPh (**9**, **10**, **11**, and **12**), the B_2 spectra show a broad region of vibrational activity from 3570 to 3700 cm^{-1}. Molecules **9** and **10** show two additional weak features at 3400 and 3500 cm^{-1}. Molecules **11** and **12** are characterized by an intense band at 3640 cm^{-1}. Gal*f*-ManSPh isomers (**13**–**16**) display more compact and similar spectra but can still be distinguished: **13** presents a low vibrational activity under 3620 cm^{-1}, **14** displays an intense band at 3640 cm^{-1}, **15** shows a weak experimental feature at 3550 cm^{-1}, and **16** displays a large feature from 3580 to 3685 cm^{-1}. Upon CID fragmentation, the four investigated trisaccharides yield the disaccharide fragment B_2 (Figure S2). Their IRMPD fingerprints were

acquired and are represented in Figure 2a (black line) for **21** (see Figures S4–S6 for **19**, **20**, and **22**). The expected correspondence is represented in green (Gal*f*-*β*-(1,4)-Man motif in Figure 2) and visual inspection shows an excellent match.

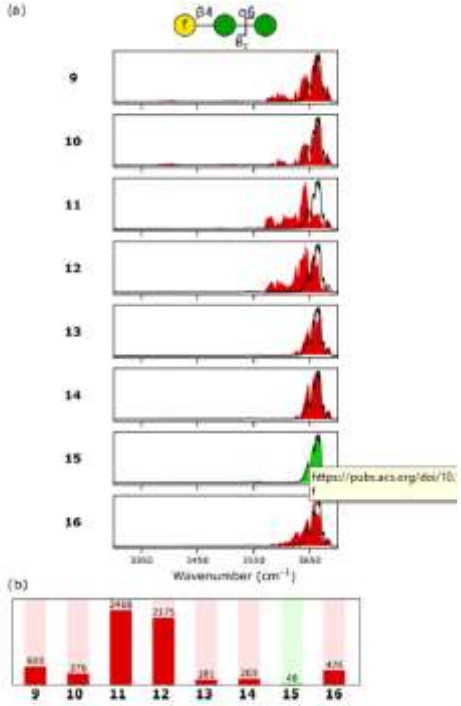

Figure 2. (a) In black, IRMPD spectrum of **21** B_2 fragments with lithium adduct. In color, IRMPD spectra of fragment m/z 331 for each Gal-ManSPh isomer. The red color corresponds to the discarded sequences and the green color to the assigned pattern. (b) Bar chart showing MSE for each reference pattern. The same color code is used.

In order to quantify this match, the mean square error (MSE) between the investigated spectrum and each spectrum of the IRMPD database was calculated as follows $MSE = c\,(\mathrm{Im}(i) - \mathrm{Id}(i))^2$ where λi is a laser wavelength in the range 3300–3700 cm^{-1}, $\mathrm{Im}(\lambda i)$ (resp. $\mathrm{Id}(\lambda i)$) is the intensity of the measured spectrum (resp. database spectrum) obtained at the wavelength λi. c is a normalization constant ($c = 33$). The best match (lowest MSE) is obtained for **15** (in green), validating that the nonreducing disaccharide fragment of **21** (Gal*f*-*β*-(1,4)-Man-*α*-(1,6)-Man) can be identified as Gal*f*-*β*-(1,4)-Man by comparing its IR fingerprint to those of a library of reference Gal-Man patterns.

The same analysis has been realized for each trisaccharide, and the MSE is presented in Figure 3. For each one, the best match corresponds to the expected Gal-Man pattern, which validates the method on B2 fragments. The method was also applied to C2 fragments (only trisaccharides 20 and 22 display C_2 fragments). The results are presented in Figures S5 and S6. For 20, the best match for the C_2 fragment was obtained for the correct sequence (Galp-*β*-(1,6)-Man). However, two candidate sequences are obtained for trisaccharide 22 due to close scores (140 and 152). In this case, the analysis of several fragments can be necessary. Therefore, the highest degree of confidence is obtained by the analysis of the B_2 fragments, which are also conveniently the most abundant ones.

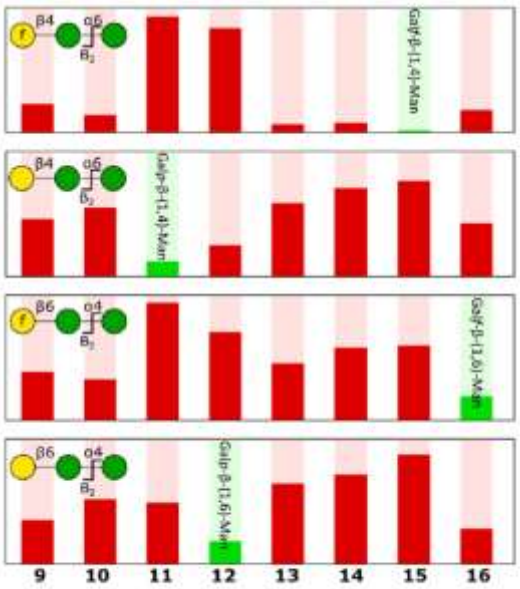

Figure 3. MSE of B2 fragments for trisaccharides **21**, **19**, **22**, and **20** (from top to bottom panel). The sequence showing the best match with the B2 fragment is represented in green and labeled.

Application: Sequencing Galactofuranose-Containing Oligosaccharide. The complete sequence coverage of oligosaccharide requires the analysis of several fragments, as illustrated in Figure 4 for trisaccharide **21**. The MS/MS spectrum of **21** features the B_2 fragment (Gal-Man nonreducing end) and the Y_2 fragment (Man-Man reducing end). The IRMPD spectrum of the B_2 fragment matches the Gal*f*-*β*-(1,4)-Man motif as described above. In the same way, the Y_2 fragment is identified as Man-*α*-(1,6)-Man (Figure S7). Therefore, the sequence Gal*f*-*β*-(1,4)-Man-*α*-(1,6)-Man is entirely recovered.

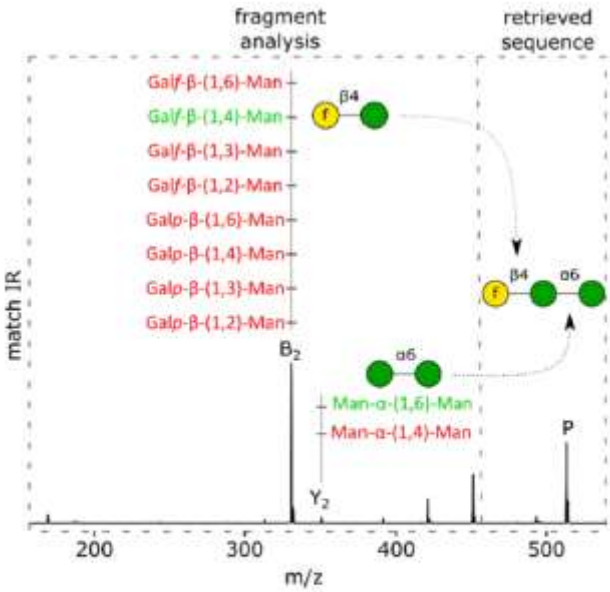

Figure 4. Sequence determination of trisaccharide **21**. Bottom: MS/MS spectrum of $[\mathbf{21} + Li]^+$. Left: B_2 (m/z 331) and Y_2 (m/z 351) fragment analyses. For both fragments, their IRMPD spectra were compared to the IRMPD spectra of reference disaccharide patterns. The pattern with the better match is in green and its structure is represented. Right: the retrieved sequence of the parent ion P (m/z 513).

We propose an intuitive representation of the IR-augmented MS sequencing in Figure 4: a scale representing the library of reference patterns is added above the fragments of interest. The results of the IRMPD analysis are reported on this scale, and the best match (lowest MSE) is highlighted in green. Finally, sequence segments are combined to retrieve the sequence of the precursor.

Application: Rapid Detection of Galactofuranose in an Oligosaccharide. Based on the B_1 fragment IRMPD spectra, we propose a novel, rapid strategy for the detection of galactofuranose-containing oligosaccharides. As illustrated in Figure 5a, an unlabeled dihexose (Gal*f*-*β*-(1,2)-Man in this example) is detected at *m/z* 349 and MS/MS produces the B_1 (galactofuranose moiety) and Z_1 (mannose moiety) signal at *m/z* 169. This signal is isolated in the ion trap and analyzed by IRMPD, yielding the IR spectrum displayed in Figure 5b. The IR spectrum of the B_1/Z_1 fragments features a distinctive signal around 3410 cm^{-1}, which indicated the presence of a galactofuranose unit. In these conditions, galactofuranosecontaining patterns can be efficiently detected without the need for chemical labeling. The patterns of interest can then be further analyzed by IRMPD for extensive structural characterization.

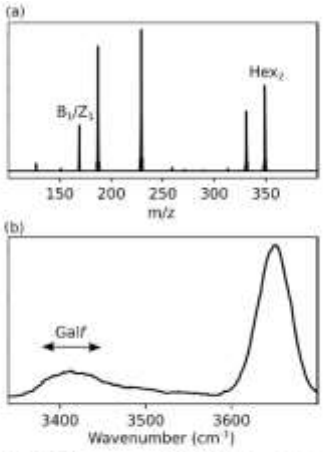

Figure 5. (a) MS/MS spectrum of unlabeled $[5 + Li]^+$. (b) IRMPD spectrum of m/z 169, which corresponds to both B_1 and Z_1 fragments. The position of the galactofuranose IR signal is marked with a double-sided arrow.

CONCLUSIONS

We demonstrated that the MS/MS fragments of galactosecontaining oligosaccharides retain the memory of the ring size of galactose, yielding diagnostic IRMPD signatures for galactofuranose and galactopyranose. This is a most surprising finding, considering the high flexibility of the furanose ring and the major molecular rearrangement occurring upon CID, particularly for the most abundant fragment (B type), where the C1−O1 bond is cleaved. A robust method for the detection of galactofuranose in an oligosaccharide is presented. It consists of the detection of a highly diagnostic band in monosaccharide fragments (3410 cm^{-1} for galactofuranose; 3510 cm^{-1} for galactopyranose), which requires only two reference spectra. At the cost of an exhaustive library of disaccharide standards, we show that both the monosaccharide content and the linkage can be derived from the IRMPD analysis of disaccharide fragments. Finally, we illustrate the

applicability of IRMPD sequencing to galactofuranose-containing oligosaccharides and propose a novel, intuitive representation of IR-augmented MS data for glycomics. All of the standards presented in this study are candidates for patterns found in lichen polysaccharides, and we expect that this study will open the way to the sequencing of polysaccharides in such exotic organisms.

ASSOCIATED CONTENT

* Supporting Information

The Supporting Information is available free of charge at https://pubs.acs.org/doi/10.1021/jacs.3c01925. Additional experimental materials (MS/MS and MS-IR) (PDF)

AUTHOR INFORMATION

Corresponding Author

Isabelle Compagnon – *CNRS, Université Claude Bernard Lyon 1, CNRS, Institut Lumie`re Matie`re, Université de Lyon, F-69622 Lyon, France;* orcid.org/0000-0003-2994-3961; Email: isabelle.compagnon@univ-lyon1.fr

Authors

Oznur Yeni – *CNRS, Université Claude Bernard Lyon 1, CNRS, Institut Lumie`re Matie`re, Université de Lyon, F-69622 Lyon, France*

Simon Ollivier – *UR BIA, F-44316 Nantes, France; INRAE, BIBS Facility, INRAE, F-44316 Nantes, France;* orcid.org/0000-0002-7671-1736

Baptiste Moge – *CNRS, Université Claude Bernard Lyon 1, CNRS, Institut Lumie`re Matie`re, Université de Lyon, F-69622 Lyon, France*

David Ropartz – *UR BIA, F-44316 Nantes, France; INRAE, BIBS Facility, INRAE, F-44316 Nantes, France;* orcid.org/0000-0003-4767-6940

Hélène Rogniaux – *UR BIA, F-44316 Nantes, France; INRAE, BIBS Facility, INRAE, F-44316 Nantes, France;* orcid.org/0000-0001-6083-2034

Laurent Legentil – *Ecole Nationale Supérieure de Chimie de Rennes, CNRS, ISCR – UMR 6226, Univ Rennes, F-35000 Rennes, France;* orcid.org/0000-0003-1402-150X

Vincent Ferrières – *Ecole Nationale Supérieure de Chimie de Rennes, CNRS, ISCR – UMR 6226, Univ Rennes, F-35000 Rennes, France;* orcid.org/0000-0002-2780-7774

Complete contact information is available at: https://pubs.acs.org/10.1021/jacs.3c01925

Funding

The authors thank the Agence Nationale de la Recherche for financially supporting the ALGAIMS project (ANR-18-CE29-0006-02, https://algaims-35.webself.net/accueil) and Region Auvergne Rhônes-Alpes for the IROLIGO grant.

Notes

The authors declare no competing financial interest.

ACKNOWLEDGMENTS

The authors thank Dr. Françoise Le Devehat and Pr. Joel Boustie for the discussion.

ABBREVIATIONS

IRMPD infrared multiple photon dissociation CID collision-induced dissociation MS mass spectrometry IR infrared ESI electrospray source ionization MSE mean square error

REFERENCES

(1) Varki, A. Biological Roles of Glycans. *Glycobiology* 2017, *27*, 3–49.

(2) Peltier, P.; Euzen, R.; Daniellou, R.; Nugier-Chauvin, C.; Ferrieres, V. Recent Knowledge and Innovations Related to Hexofuranosides: Structure, Synthesis and Applications. *Carbohydr. Res.* 2008, *343*, 1897–1923.

(3) Richards, M. R.; Lowary, T. L. Chemistry and Biology of Galactofuranose-Containing Polysaccharides. *ChemBioChem* 2009, *10*, 1920–1938.

(4) Szamosvari, D.; Bae, M.; Bang, S.; Tusi, B. K.; Cassilly, C. D.; Park, S.-M.; Graham, D. B.; Xavier, R. J.; Clardy, J. Lyme Disease, *Borrelia burgdorferi*, and Lipid Immunogens. *J. Am. Chem. Soc.* 2022, *144*, 2474–2478.

(5) Tefsen, B.; Ram, A. F.; van Die, I.; Routier, F. H. Galactofuranose in Eukaryotes: Aspects of Biosynthesis and Functional Impact. *Glycobiology* 2012, *22*, 456–469.

(6) Schmalhorst, P. S.; Krappmann, S.; Vervecken, W.; Rohde, M.; Mu¨ller, M.; Braus, G. H.; Contreras, R.; Braun, A.; Bakker, H.; Routier, F. H. Contribution of Galactofuranose to the Virulence of the Opportunistic Pathogen Aspergillus Fumigatus. *Eukaryot. Cell* 2008, *7*, 1268–1277.

(7) Whitfield, C.; Richards, J. C.; Perry, M. B.; Clarke, B. R.; MacLean, L. L. Expression of Two Structurally Distinct D-Galactan O Antigens in the Lipopolysaccharide of Klebsiella Pneumoniae Serotype O1. *J. Bacteriol.* 1991, *173*, 1420–1431.

(8) Leitao, E. A. Galactofuranose-Containing O-Linked Oligosaccharides Present in the Cell Wall Peptidogalactomannan of Aspergillus Fumigatus Contain Immunodominant Epitopes. *Glycobiology* 2003, *13*, 681–692.

(9) San-Blas, G.; Prieto, A.; Bernabe, M.; Ahrazem, O.; Moreno, B.; Leal, J. A. α-Galf 1 → 6-α-Mannopyranoside Side Chains in Paracoccidioides Brasiliensis Cell Wall Are Shared by Members of the Onygenales, but Not by Galactomannans of Other Fungal Genera. *Med. Mycol.* 2005, *43*, 153–159.

(10) Carbonero, E. R.; Cordeiro, L. M. C.; Mellinger, C. G.; Sassaki, G. L.; Stocker-Worgotter, E.; J Gorin, P. A.; Iacomini, M. Galactomannans with Novel Structures from the Lichen *Roccella Decipiens* Darb. *Carbohydr. Res.* 2005, *340*, 1699−1705.
(11) Gorin, P. A.; Iacomini, M. STRUCTURAL DIVERSITY OF DGALACTO-D-MANNAN COMPONENTS ISOLATED FROM LICHENS HAVING ASCOMYCETOUS MYCOSYMBIONTS. *Carbohydr. Res.* 1985, *142*, 253−267.
(12) Sone, Y.; Isoda-Johmura, M.; Misaki, A. Isolation and Chemical Characterization of Polysaccharides from Iwatake, *Gyrophora esculenta* Miyoshi. *Biosci. Biotechnol. Biochem.* 1996, *60*, 213−215.
(13) Carbonero, E. R.; Smiderle, F. R.; Gracher, A. H. P.; Mellinger, C. G.; Torri, G.; Ahti, T.; Gorin, P. A. J.; Iacomini, M. Structure of Two Glucans and a Galactofuranomannan from the Lichen Umbilicaria Mammulata. *Carbohydr. Polym.* 2006, *63*, 13−18.
(14) Ho, J. S.; Gharbi, A.; Schindler, B.; Yeni, O.; Bredy, R.; Legentil, L.; Ferrie`res, V.; Kiessling, L. L.; Compagnon, I. Distinguishing Galactoside Isomers with Mass Spectrometry and Gas-Phase Infrared Spectroscopy. *J. Am. Chem. Soc.* 2021, *143*, 10509−10513.
(15) Favreau, B.; Yeni, O.; Ollivier, S.; Boustie, J.; Devehat, F. L.; Guegan, J.-P.; Fanuel, M.; Rogniaux, H.; Bredy, R.; Compagnon, I.; Ropartz, D.; Legentil, L.; Ferrie`res, V. Synthesis of an Exhaustive Library of Naturally Occurring Galf-Manp and Galp-Manp Disaccharides. Toward Fingerprinting According to Ring Size by Advanced Mass Spectrometry-Based IM-MS and IRMPD. *J. Org. Chem.* 2021, *86*, 6390−6405.
(16) Gandolfi-Donadio, L.; Gallo-Rodriguez, C.; de Lederkremer, R. M. Synthesis of α-d-Galp-(1 → 3)-β-d-Galf-(1 → 3)-d-Man, a Terminal Trisaccharide of Leishmania Type-2 Glycoinositolphospholipids. *J. Org. Chem.* 2002, *67*, 4430−4435.
(17) Li, T.-R.; Piccini, G.; Tiefenbacher, K. Supramolecular Capsule-Catalyzed Highly β-Selective Furanosylation Independent of the S_N1/S_N2 Reaction Pathway. *J. Am. Chem. Soc.* 2023, *145*, 4294−4303.
(18) Bai, Y.; Lowary, T. L. 2,3-Anhydrosugars in Glycoside Bond Synthesis. Application to α-D-Galactofuranosides. *J. Org. Chem.* 2006, *71*, 9658−9671.
(19) Lee, Y. J.; Lee, B.-Y.; Jeon, H. B.; Kim, K. S. Total Synthesis of Agelagalastatin. *Org. Lett.* 2006, *8*, 3971−3974.
(20) Thomann, J.-S.; Monneaux, F.; Creusat, G.; Spanedda, M. V.; Heurtault, B.; Habermacher, C.; Schuber, F.; Bourel-Bonnet, L.; Frisch, B. Novel Glycolipid TLR2 Ligands of the Type Pam2Cys-α-Gal: Synthesis and Biological Properties. *Eur. J. Med. Chem.* 2012, *51*, 174−183.
(21) Both, P.; Green, A. P.; Gray, C. J.; Sˇardzik, R.; Voglmeir, J.;

Fontana, C.; Austeri, M.; Rejzek, M.; Richardson, D.; Field, R. A.; Widmalm, G.; Flitsch, S. L.; Eyers, C. E. Discrimination of Epimeric Glycans and Glycopeptides Using IM-MS and Its Potential for Carbohydrate Sequencing. *Nat. Chem.* 2014, *6*, 65−74.
(22) Gray, C. J.; Thomas, B.; Upton, R.; Migas, L. G.; Eyers, C. E.; Barran, P. E.; Flitsch, S. L. Applications of Ion Mobility Mass Spectrometry for High Throughput, High Resolution Glycan Analysis. *Biochim. Biophys. Acta, Gen. Subj.* 2016, *1860*, 1688−1709.
(23) Gray, C. J.; Schindler, B.; Migas, L. G.; Picˇmanova, M.; Allouche, A. R.; Green, A. P.; Mandal, S.; Motawia, M. S.; Sanchez-Perez, R.; Bjarnholt, N.; Moller, B. L.; Rijs, A. M.; Barran, P. E.; Compagnon, I.; Eyers, C. E.; Flitsch, S. L. Bottom-Up Elucidation of Glycosidic Bond Stereochemistry. *Anal. Chem.* 2017, *89*, 4540−4549.
(24) Ben Faleh, A.; Warnke, S.; Rizzo, T. R. Combining Ultrahigh-Resolution Ion-Mobility Spectrometry with Cryogenic Infrared Spectroscopy for the Analysis of Glycan Mixtures. *Anal. Chem.* 2019, *91*, 4876−4882.
(25) Grabarics, M.; Lettow, M.; Kirschbaum, C.; Greis, K.; Manz, C.; Pagel, K. Mass Spectrometry-Based Techniques to Elucidate the Sugar Code. *Chem. Rev.* 2022, *122*, 7840−7908.
(26) Gray, C. J.; Migas, L. G.; Barran, P. E.; Pagel, K.; Seeberger, P. H.; Eyers, C. E.; Boons, G.-J.; Pohl, N. L. B.; Compagnon, I.; Widmalm, G.; Flitsch, S. L. Advancing Solutions to the Carbohydrate Sequencing Challenge. *J. Am. Chem. Soc.* 2019, *141*, 14463−14479.
(27) Mucha, E.; Marianski, M.; Xu, F.-F.; Thomas, D. A.; Meijer, G.; von Helden, G.; Seeberger, P. H.; Pagel, K. Unravelling the Structure of Glycosyl Cations via Cold-Ion Infrared Spectroscopy. *Nat. Commun.* 2018, *9*, No. 4174.
(28) Elferink, H.; Severijnen, M. E.; Martens, J.; Mensink, R. A.; Berden, G.; Oomens, J.; Rutjes, F. P. J. T.; Rijs, A. M.; Boltje, T. J. Direct Experimental Characterization of Glycosyl Cations by Infrared Ion Spectroscopy. *J. Am. Chem. Soc.* 2018, *140*, 6034−6038.
(29) Mucha, E.; Gonzalez Florez, A. I.; Marianski, M.; Thomas, D. A.; Hoffmann, W.; Struwe, W. B.; Hahm, H. S.; Gewinner, S.; Schollkopf, W.; Seeberger, P. H.; von Helden, G.; Pagel, K. Glycan Fingerprinting via Cold-Ion Infrared Spectroscopy. *Angew. Chem., Int. Ed.* 2017, *56*, 11248−11251.
(30) Masellis, C.; Khanal, N.; Kamrath, M. Z.; Clemmer, D. E.; Rizzo, T. R. Cryogenic Vibrational Spectroscopy Provides Unique Fingerprints for Glycan Identification. *J. Am. Soc. Mass Spectrom.* 2017, *28*, 2217−2222.
(31) Warnke, S.; Ben Faleh, A.; Scutelnic, V.; Rizzo, T. R. Separation and Identification of Glycan Anomers Using Ultrahigh-Resolution Ion-Mobility Spectrometry and Cryogenic Ion Spectroscopy. *J. Am. Soc. Mass Spectrom.* 2019, *30*, 2204−2211.
(32) Schindler, B.; Barnes, L.; Renois, G.; Gray, C.; Chambert, S.;

Fort, S.; Flitsch, S.; Loison, C.; Allouche, A.-R.; Compagnon, I. Anomeric Memory of the Glycosidic Bond upon Fragmentation and Its Consequences for Carbohydrate Sequencing. *Nat. Commun.* 2017, *8*, No. 973.
(33) Schindler, B.; Barnes, L.; Gray, C. J.; Chambert, S.; Flitsch, S. L.; Oomens, J.; Daniel, R.; Allouche, A. R.; Compagnon, I. IRMPD Spectroscopy Sheds New (Infrared) Light on the Sulfate Pattern of Carbohydrates. *J. Phys. Chem. A* 2017, *121*, 2114−2120.
(34) Tan, Y.; Polfer, N. C. Linkage and Anomeric Differentiation in Trisaccharides by Sequential Fragmentation and Variable-Wavelength Infrared Photodissociation. *J. Am. Soc. Mass Spectrom.* 2015, *26*, 359−368.
(35) Schindler, B.; Joshi, J.; Allouche, A.-R.; Simon, D.; Chambert, S.; Brites, V.; Gaigeot, M.-P.; Compagnon, I. Distinguishing Isobaric Phosphated and Sulfated Carbohydrates by Coupling of Mass Spectrometry with Gas Phase Vibrational Spectroscopy. *Phys. Chem. Chem. Phys.* 2014, *16*, 22131−22138.
(36) Taha, H. A.; Richards, M. R.; Lowary, T. L. Conformational Analysis of Furanoside-Containing Mono- and Oligosaccharides. *Chem. Rev.* 2013, *113*, 1851−1876.
(37) Schindler, B.; Legentil, L.; Allouche, A.-R.; Ferrie`res, V.; Compagnon, I. Spectroscopic Diagnostic for the Ring-Size of Carbohydrates in the Gas Phase: Furanose and Pyranose Forms of GalNAc. *Phys. Chem. Chem. Phys.* 2019, *21*, 12460−12467.
(38) Laine, R. A. Invited Commentary: A Calculation of All Possible Oligosaccharide Isomers Both Branched and Linear Yields 1.05 × 1012 Structures for a Reducing Hexasaccharide: The Isomer Barrier to Development of Single-Method Saccharide Sequencing or Synthesis Systems. *Glycobiology* 1994, *4*, 759−767.
(39) Ollivier, S.; Legentil, L.; Yeni, O.; David, L.-P.; Ferrie`res, V.; Compagnon, I.; Rogniaux, H.; Ropartz, D. Gas-Phase Behavior of Galactofuranosides upon Collisional Fragmentation: A Multistage High-Resolution Ion Mobility Study. *J. Am. Soc. Mass Spectrom.* 2023, *34*, 627−639.
(40) Schindler, B.; Laloy-Borgna, G.; Barnes, L.; Allouche, A.-R.; Bouju, E.; Dugas, V.; Demesmay, C.; Compagnon, I. Online Separation and Identification of Isomers Using Infrared Multiple Photon Dissociation Ion Spectroscopy Coupled to Liquid Chromatography: Application to the Analysis of Disaccharides Regio-Isomers and Monosaccharide Anomers. *Anal. Chem.* 2018, *90*, 11741−11745.
(41) Domon, B.; Costello, C. E. A Systematic Nomenclature for Carbohydrate Fragmentations in FAB-MS/MS Spectra of Glycoconjugates. *Glycoconjugate J.* 1988, *5*, 397−409.